The EMBO Journal vol.15 no.12 pp.2935–2943, 1996

Myristoylated and non-myristoylated forms of the pH sensor protein hisactophilin II: intracellular shuttling to plasma membrane and nucleus monitored in real time by a fusion with green fluorescent protein

Frank Hanakam[1], Richard Albrecht, Christoph Eckerskorn, Monika Matzner and Günther Gerisch

Max-Planck-Institut für Biochemie, D-82152 Martinsried, Germany

[1]Corresponding author

Hisactophilins are myristoylated proteins that are rich in histidine residues and known to exist in *Dictyostelium* cells in a plasma membrane-bound and a soluble cytoplasmic state. Intracellular translocation of these proteins in response to pH changes was monitored using hisactophilin fusions with green fluorescent protein (GFP) and confocal laser scanning microscopy. Both the normal and a mutated non-myristoylated fusion protein shuttled within the cells in a pH-dependent manner. After lowering the pH, these proteins translocated within minutes between the cytoplasm, the plasma membrane and the nucleus. The role of histidine clusters on the surface of hisactophilin molecules in binding of the proteins to the plasma membrane and in their transfer to the nucleus is discussed on the basis of a pH switch mechanism.

Keywords: actin binding proteins/*Dictyostelium*/histidine-rich proteins/nuclear translocation signals/protein–lipid interactions

Introduction

Hisactophilins I and II are small actin and membrane binding proteins of *Dictyostelium discoideum* that are myristoylated at their N-terminus (Scheel *et al.*, 1989; Hanakam *et al.*, 1995). These proteins are characterized by a high content of 31–35 histidine residues which are clustered in loops on the surface of the molecules (Habazettl *et al.*, 1992). The binding of hisactophilins to actin and acidic lipids is sharply pH dependent within the range of cytoplasmic pH variations, in accord with a p*K* of 6.5 of histidine residues. At pH ≤6.5 but not at pH 7.5, hisactophilins efficiently associate with actin (Scheel *et al.*, 1989). Similarly, the binding of hisactophilin II to monolayers of acidic lipids is greatly altered by pH (Behrisch *et al.*, 1995; Hanakam *et al.*, 1996).

A variety of the myristoylated proteins of eukaryotic cells shuttle between the cytoplasm and the inner phase of the plasma membrane (Resh, 1994). In some of these proteins, membrane binding is mediated by the combined effect of the fatty acid and positively charged amino acids. The myristoyl residue inserts into the inner lipid layer of the plasma membrane (Vergères *et al.*, 1995), and clusters of basic amino acids interact with acidic membrane lipids (Kim *et al.*, 1991, 1994). Lysine residues are often clustered close to the myristoylated N-terminus of the proteins (Resh, 1994). Membrane binding of myristoylated or farnesylated proteins can be switched off by the phosphorylation of serine or threonine residues that are interspersed between the clusters of basic amino acids (Swierczynski and Blackshear, 1995). Other myristoylated proteins switch upon ligand binding. For instance, the retinal protein recoverin translocates to a lipid bilayer in response to Ca^{2+} binding (Tanaka *et al.*, 1995), and GTP (or GTPγS) affects the conformation of ADP-ribosylation factor 1 (Randazzo *et al.*, 1995). The myristoyl residue may also bind to a hydrophobic pocket and thus convey structural stability to a protein (Zheng *et al.*, 1993).

Here we provide evidence for a switch mechanism which is operated by cytoplasmic pH changes. In order to monitor pH-dependent protein shuttling within living cells, hisactophilin II was engineered and expressed with a tag of the green fluorescent protein (GFP) from the jelly fish, *Aequorea victoria* (Prasher *et al.*, 1992; Chalfie *et al.*, 1994).

The strong pH dependence of the surface charge of hisactophilins makes it possible to manipulate it from outside the cell by pH clamping within the physiological range. In order to separate the effect of surface charges on the protein moiety from influences of the myristoyl residue, the N-terminal glycine residue was converted into alanine. The Gly→Ala conversion is known to prevent myristoylation in mammalian proteins (Swierczynski and Blackshear, 1995). Fusions of mutated hisactophilin II with GFP were constructed in order to compare their intracellular distribution with the localization of normal, myristoylated hisactophilin II–GFP fusions.

Results

Expression of hisactophilin II–GFP fusions in Dictyostelium cells

Figure 1 shows the constructions made to express myristoylated and non-myristoylated fusions of hisactophilin II and GFP in *D.discoideum*. The normal version of the fusion protein is designated as Gly^2-HsII–GFP, the mutated form as Ala^2-HsII–GFP. (Methionine as the first residue is cleaved off from the mature protein.) Cells of *D.discoideum* were transfected with vectors that integrate into the genome and carry the coding region of the fusion proteins under control of the strong actin 15 promoter (Cohen *et al.*, 1986). Both the Gly^2 and Ala^2 fusion proteins were ~6-fold overexpressed relative to the sum of the endogenous hisactophilins I and II (Figure 1A). For analytical purposes and for the assay of actin binding, the fusion proteins were purified from the soluble fraction of *D.discoideum* cell lysates. Fractionation according to hydrophobicity yielded two peaks of Gly^2-HsII–GFP (Figure 1B), which were analysed by mass spectrometry.

The more hydrophilic protein of the first peak had a mass of 41 432 ± 3 Da in accord with the calculated mass of the unmodified fusion protein. The protein of the more hydrophobic fraction had a mass of 41 642 ± 3 Da, indicating that it is modified by a myristoyl residue of 210 Da. The ratio of the myristoylated to the unmodified form was 6:4 in the preparation shown in Figure 1B. This ratio may depend on the degree of overexpression and may be higher in the membrane-bound fraction than in the cytosolic one. The results show, in any case, that the increased rate of synthesis of the protein exceeds the capacity of the myristoylation system.

The mutated fusion protein Ala^2-HsII–GFP showed only one peak, almost coinciding with the unmodified form of Gly^2-HsII–GFP (Figure 1B). The mass of this protein was 41 482 ± 3 Da, showing the absence of myristoylation. This mass suggests the presence of an acetyl residue (Figure 1C), in accord with the finding that the N-terminus is blocked.

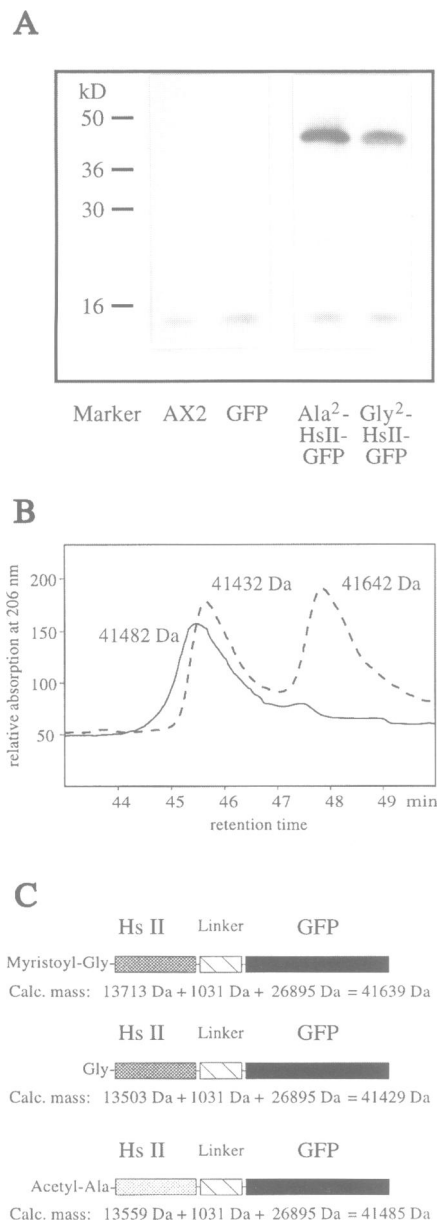

pH-dependent actin binding shows that the hisactophilin–GFP fusions are functional

Hisactophilin was identified initially as a protein that binds to actin in a pH-dependent manner (Scheel *et al.*, 1989). In order to verify that the fusion proteins are in an active conformation and that the presence of the GFP moiety does not interfere with the binding of hisactophilin to actin, co-sedimentation assays were performed. The HsII–GFP fusions were added to G-actin and, after polymerization, the incubation mixtures were centrifuged at 100 000 *g* to sediment the F-actin. As a measure of co-sedimentation, fluorescence in the pellet fractions was determined (Figure 2). Both fusion proteins co-sedimented with F-actin at pH values <7.0, with half-maximal co-sedimentation at pH 6.5, coincident with the isoelectric point of histidine residues. No significant co-sedimentation of the fusion proteins with F-actin was obtained at pH >7.0, nor was co-sedimentation observed in a control with free GFP and F-actin at the permissive pH of 6.1.

pH-dependent re-distribution of hisactophilins between the cytoplasm, plasma membrane and nucleus

Extensive re-distribution of hisactophilins was observed by pH clamping of *D.discoideum* cells. Wild-type cells were subjected to buffers of different pH in the presence of a weak acid or base. Both propionic acid and ammonia can diffuse through the plasma membrane in their undissociated state and, after dissociation within the cells, alter the pH of the cytoplasm (Inouye, 1989). After fixation, the cells were labelled with mAb 54-11-10 which recognizes both hisactophilin I and II (Hanakam *et al.*, 1995). Immunofluorescence images showed a brilliant label at the plasma membrane and within the nuclei of cells that had been incubated with 10 mM propionic acid at pH 6.0 (Figure 3A and B). The membrane label appeared to be patchy, indicating that the hisactophilins were strongly clustered beneath the cell surface. In cells incubated with 5 mM ammonium chloride at pH 8.0, the plasma membrane was labelled less prominently and more uniformly (Figure

Fig. 1. Hisactophilin II–GFP fusion proteins and their modifications in *D.discoideum* cells. Cells of strain AX2 were transfected with vectors encoding either GFP, Ala^2-HsII–GFP or Gly^2-HsII–GFP, and the proteins produced in transfected and control cells were analysed. (**A**) Immunoblot of total proteins from growth-phase cells labelled with hisactophilin-specific mAb 54-11-10. In untransformed cells (AX2) and cells producing free GFP, only the band representing the two 14 kDa isoforms of endogenous hisactophilin is labelled. In cells producing Ala^2- or Gly^2-HsII–GFP fusion proteins, these 41/42 kDa proteins are recognized by the same antibody as strongly labelled bands in addition to the free hisactophilins. (**B**) Analysis by reversed-phase HPLC of fusion proteins purified from the cytosol of transfected cells that produce either Ala^2-HsII–GFP (solid line) or Gly^2-HsII–GFP (dashed line). The indicated sizes of proteins in the peaks were determined by electrospray ionization mass spectrometry (ESI-MS). (**C**) Diagram of fusion proteins in which normal or mutated hisactophilin II sequences (dotted) are linked through a flexible $(GlyGlySer)_4$ spacer (hatched) to the GFP polypeptide chain (filled). Calculation of the mass of GFP is based on the sequence reported by Prasher *et al.* (1992) with codon 80 giving rise to arginine (Chalfie *et al.*, 1994). Assuming acetylation for the blocked N-terminus of the Ala^2 variant, the calculated sizes for the modified and unmodified fusion proteins were in agreement with those determined by ESI-MS. With respect to the Gly^2-HsII–GFP construct, masses were calculated for the unmodified and the myristoylated protein to account for the two protein peaks resolved in (B).

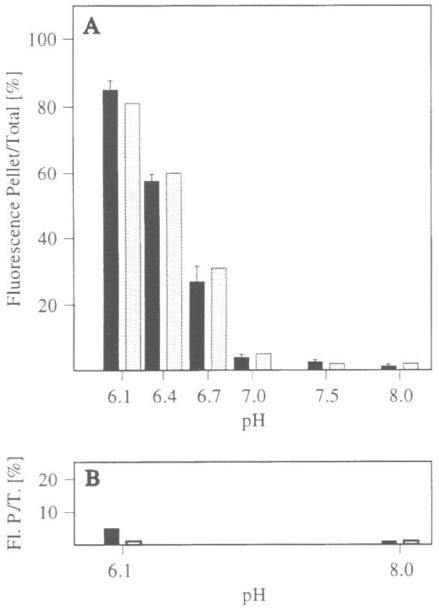

Fig. 2. Ability of fusion proteins to co-sediment with actin filaments in the pH-dependent manner typical of hisactophilins. (**A**) Co-sedimentation of Gly^2-HsII–GFP (filled bars) and Ala^2-HsII–GFP (shaded bars) with F-actin at pH 6.1–8.0. (**B**) Two controls, one showing sedimentation of Gly^2-HsII–GFP without actin (filled) the other free GFP together with actin (shaded).

3C). The cytoplasm was labelled throughout, and the nuclei were not distinct from the cytoplasm.

The fluorescence images showing accumulation of hisactophilins at the border of the cells do not have the spatial resolution necessary to distinguish binding to the inner membrane surface from association with the actin-rich cell cortex. To distinguish between these possibilities by electron microscopy, we have employed immunogold labelling of cryosections with mAb 54-11-10. This antibody localized the endogenous hisactophilins I and II to a shallow layer at the cell boundary, indicating their immediate association with the plasma membrane (Figure 4A). In contrast, labelling with an anti-actin antibody that recognizes both monomeric and filamentous actin revealed the enrichment of actin in a cortical layer of varying thickness of the order of 100 nm (Figure 4B).

Shuttling of myristoylated and non-myristoylated hisactophilin II–GFP between the cytoplasm and the plasma membrane

Living cells of *D.discoideum* producing either Gly^2-HsII–GFP or Ala^2-HsII–GFP showed a strong green fluorescence. The re-distribution of HsII–GFP obtained by pH clamping largely reflected the localization of endogenous hisactophilins I and II. The first panel of Figure 5 shows confocal images of a single Gly^2-HsII–GFP-producing cell consecutively exposed to low and high pH conditions. In buffer pH 6.0, the fusion protein was located primarily in the cytoplasmic space. Upon addition of propionic acid adjusted to the same pH, the cytoplasm was largely depleted of the protein which accumulated at the plasma membrane and in the nucleus. This re-localization was reversible upon increasing the pH with the addition of 5 mM ammonium chloride.

To investigate whether the myristoyl residue on the N-terminus of the protein is necessary for membrane association, cells producing Ala^2-HsII–GFP were exposed to the same sequence of pH conditions as cells producing Gly^2-HsII–GFP. Strong accumulation of Ala^2-HsII–GFP at the plasma membrane and also in the nucleus was observed at pH 6.0 in the presence of propionic acid, and re-localization to the cytoplasm at pH 8.0 was obtained with ammonium chloride (Figure 5, middle panel). Control cells producing free GFP showed intense fluorescence in

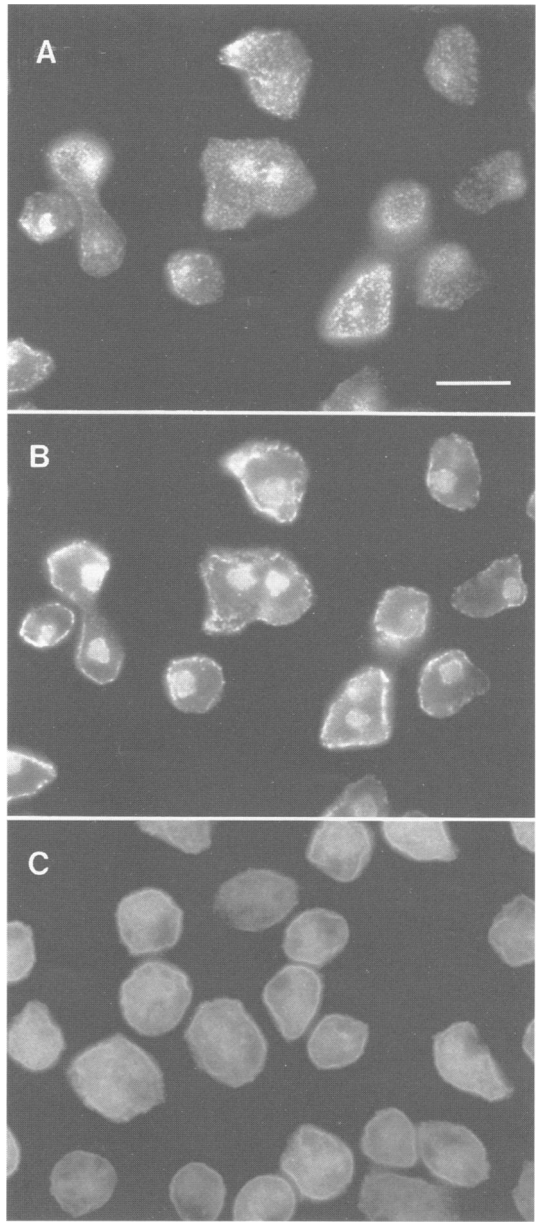

Fig. 3. pH-dependent re-distribution of endogenous hisactophilins I and II. Prior to fixation, wild-type cells were exposed for 10 min to 10 mM propionic acid at pH 6.0 (A and B) or to 5 mM ammonium chloride at pH 8.0 (C). The hisactophilins were localized by immunofluorescence labelling with mAb 54-11-10 followed by TRITC-conjugated goat anti-mouse immunoglobulin antibody. In the presence of propionic acid, hisactophilins were clustered at the plasma membrane, most clearly seen by focusing to the plane of contact of the cells with the glass coverslip (**A**), and they accumulated in the nuclei, as recognized by focusing to the centre of the cells (**B**). Upon treatment with ammonia and focusing as in (B), the cells showed a weaker and more uniform accumulation of hisactophilins at the plasma membrane, higher concentrations in the cytoplasm and no apparent enrichment in the nuclei (**C**). Bar: 10 μm.

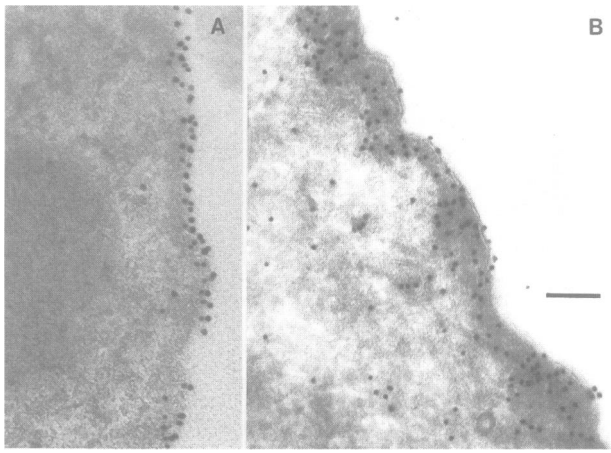

Fig. 4. Cortical regions of cells immunogold labelled with anti-hisactophilin antibody (**A**) or anti-actin antibody (**B**). Before fixation and embedding for cryosectioning, the cells had been exposed to 10 mM propionic acid at pH 6.0. Cryosections were incubated with mAb 54-11-10 for (A) or with mAb 224-236-1 for (B), subsequently with rabbit anti-mouse immunoglobulin antibody, and finally labelled with protein A conjugated to 10 nm gold. Bar: 100 nm.

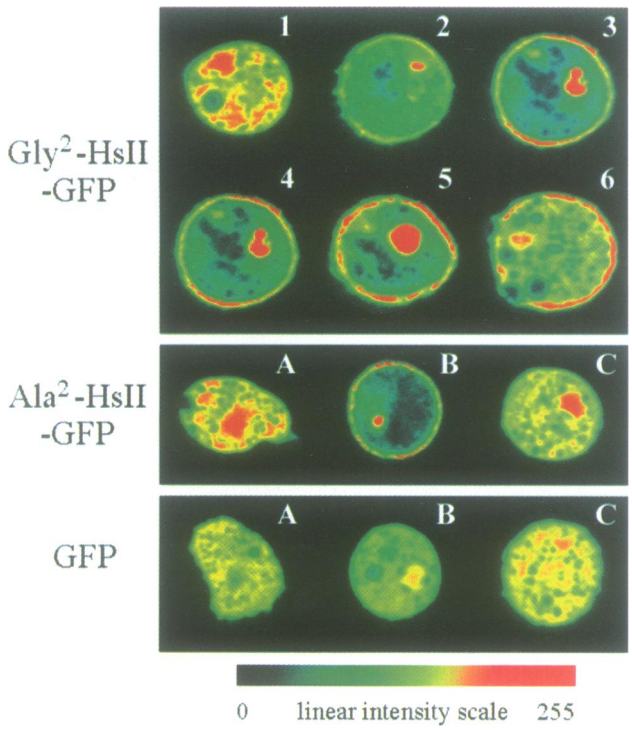

Fig. 5. pH-induced intracellular re-distribution of Gly^2-HsII–GFP (top panel) and Ala^2-HsII–GFP (middle panel), in comparison with free GFP (bottom panel). Increasing fluorescence emission is represented by false colours from dark green to red. Top panel: a single cell producing Gly^2-HsII–GFP subjected consecutively to 20 mM MES buffer, pH 6.0 (frame 1), to the same buffer plus 10 mM propionic acid adjusted to pH 6.0 (frames 2–4) and finally to medium partially replaced by 20 mM Tris buffer, pH 8.0, supplemented with 10 mM ammonium chloride (frames 5–6), which raised the external pH to ~7.3. The images demonstrate that the weak acid causes reversible accumulation of the fusion protein at the plasma membrane and in the nucleus. Middle and bottom panels: representative cells producing either Ala^2-HsII–GFP (middle) or GFP (bottom). (A) 20 mM MES buffer pH 6.0; (B) 10 min after the addition of 10 mM propionic acid, pH 6.0; (C) 10 min after partial replacement of the medium by 20 mM Tris buffer containing 10 mM ammonium chloride, resulting in a pH of ~7.3.

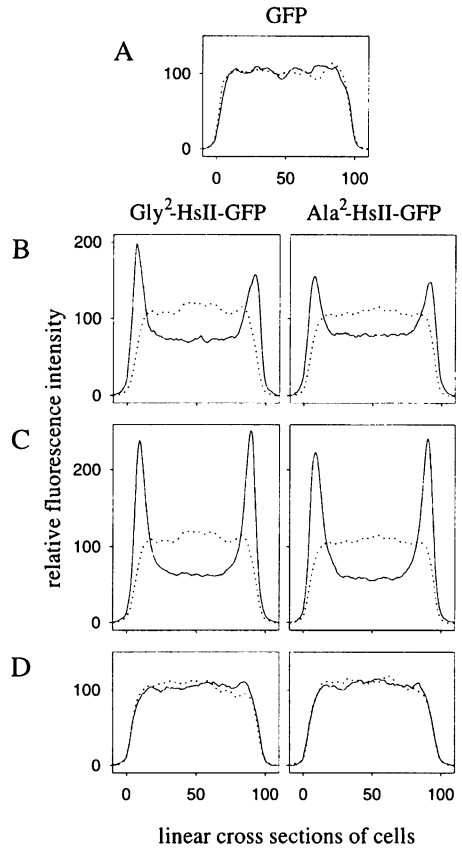

Fig. 6. Distribution of GFP (A) and fusion proteins (B–D) between the cytoplasm and surface regions of cells subjected to different pH conditions. (**A** and **B**) Cells incubated for 10 min in either 20 mM MES buffer with 10 mM propionic acid, pH 6.0 (solid lines) or 20 mM Tris buffer with 5 mM ammonium chloride, pH 8.0 (dotted lines). (**C**) Cells incubated for 10 min in the MES buffer with 20 mM propionic acid, pH 6.0 (solid lines) or in the Tris buffer with ammonium chloride, pH 8.0 (dotted reference lines, the same as in B). (**D**) Cells incubated in either 20 mM MES buffer, pH 6.0 (solid lines) or 20 mM Tris buffer, pH 8.0 without any additions (dotted lines).

the cytoplasm without a detectable increase at the plasma membrane at any pH. At pH 6.0 with propionic acid in the buffer, weak accumulation of GFP in the nucleus was observed (Figure 5, lower panel).

The results exemplified in Figure 5 were substantiated by the quantitative analysis of fluorescence profiles using confocal microscopy and averaging of data collected in a population of cells. Figure 6 shows line scans normalized with respect to total fluorescence intensities and to sizes of the cells. In cells incubated with propionic acid at pH 6.0, both Gly^2- and Ala^2-HsII–GFP exhibited sharp peaks of fluorescence intensity at the cell borders (Figure 6B and C). These peaks were not seen at pH 8.0 in the presence of 5 mM ammonium chloride or in buffer without any additions (Figure 6D).

Although the pattern of HsII–GFP re-distribution is, in general, consistent with predictions that are based on the locations of endogenous hisactophilins in cells exposed to propionic acid or ammonia (Figure 3), there is one difference. No enrichment of HsII–GFP on the plasma membrane was detected in the presence of ammonia (Figure 5, upper panel, and Figure 6), whereas the endogenous hisactophilins remained detectable at the plasma membrane even when the pH was higher than used for

HsII–GFP (Figure 3C). The most likely explanation for this difference resides in the overexpression of HsII–GFP superimposed on normal levels of endogenous hisactophilins. If one assumes that hisactophilin binding to the membrane is saturable, a strong increase in the ratio of cytoplasmic to membrane-bound hisactophilin would be a consequence of overexpression. In any case, free GFP showed uniform distribution within the control cells, confirming that membrane association of the fusion proteins is due to their hisactophilin moieties (Figure 6A).

The dynamics of shuttling between cytoplasm and membrane were investigated by changing the extracellular medium while continuously imaging the fluorescence of Gly^2-HsII–GFP in a group of cells. Within 1–2 min after the addition of propionic acid at pH 6.0, the protein substantially accumulated at the plasma membrane until it came close to a steady-state level after 5–10 min (Figure 7). The reversibility of the translocation was demonstrated by adding ammonium chloride at pH 7.3. The fusion protein separated from the membrane and accumulated in the cytoplasm on a time scale similar to that with which it associated with the membrane.

A pH switch controls bidirectional shuttling of hisactophilin between cytoplasm and nucleus

As Figure 5 revealed, HsII–GFP was translocated at low pH not only to the plasma membrane but also to the nucleus. Strong patchy labelling in the periphery of the intranuclear space suggested that the fusion protein was most strongly enriched in the nucleoli. In *Dictyostelium* cells, the nucleoli are attached to the inner layer of the nuclear membrane (Fukui, 1978). These nucleoli are easily identified as lensiform dark bodies by phase-contrast optics. In order to confirm the intranuclear localization and to exclude an artifact due to the GFP moiety, we have labelled the endogenous hisactophilins in cryosections of *D.discoideum* cells by immunogold for electron microscopy. Figure 8 shows the accumulation of hisactophilins within the nucleus of cells treated with propionic acid at pH 6.0. The hisactophilins were enriched in the nuclear matrix (Figure 8A), and were accumulated more strongly in the nucleoli (Figure 8B). As a control, cells were incubated in parallel with anti-actin antibody. This antibody, which strongly labelled the cell cortex, showed no significant labelling of the nucleoli (Figure 8C).

The kinetics of entry into the nucleus and exit into the cytoplasm were followed by line scans through the nuclear region of cells exposed to changing pH conditions. As exemplified in Figure 9, the entry of HsII–GFP fusion proteins was already detectable within 1 min of lowering the pH. Only a few minutes were required for re-distribution to the cytoplasm after raising the pH.

Discussion

Role of charges in hisactophilin–membrane binding in vivo

The results obtained with the Ala^2-HsII–GFP construct show that hisactophilin II differs from the majority of myristoylated proteins (McLaughlin and Aderem, 1995) in that it translocates in a pH-dependent manner to the plasma membrane and does not require the myristoyl residue for membrane association. This behaviour is in agreement with data showing similarly strong binding of myristoylated and non-myristoylated hisactophilins to negatively charged lipid monolayers that contain dimyristoylphosphatidylglycerol (Behrisch *et al.*, 1995). The binding of hisactophilins to negatively charged lipids is extremely pH dependent in the range of pH 6.5–7.5, indicating that the binding depends on positively charged histidine residues. The myristoyl residue is essential for the association of hisactophilins with neutral lipids (A.Seelig, personal communication), and it strengthens a decrease in the lateral diffusion of lipids to which hisactophilin is attached (Behrisch *et al.*, 1995). Although the fatty acid is not required in living cells for binding to the plasma membrane, it might play a critical role in orientating the protein relative to a membrane surface, as suggested by Hanakam *et al.* (1995), and in the coupling of actin to a membrane (Behrisch *et al.*, 1995).

According to the immunolabel shown in Figure 4, membrane binding in living cells appears to override the interaction of hisactophilins with actin filaments. However, this finding does not exclude the possibility that hisactophilin interacts with actin *in vivo*, as it does *in vitro* (Scheel *et al.*, 1989). The epitope to which the monoclonal antibody binds might be occupied in hisactophilin–actin complexes. Like filamin (Nunnally and Craig, 1980), talin (Schmidt *et al.*, 1993) and ABP-50 (Edmonds *et al.*, 1995), three other proteins whose interaction with actin filaments critically depends on pH, hisactophilins might play a role in stabilizing the actin network in the cell cortex when the cytoplasmic pH decreases below 7.0.

pH switch controlling hisactophilin localization to the nucleus

Our data show that hisactophilin–GFP fusions are valuable tools for studying the reversible translocation of proteins into the nucleus of living cells. Despite the fact that GFP has twice the mass of hisactophilin, the fusion proteins

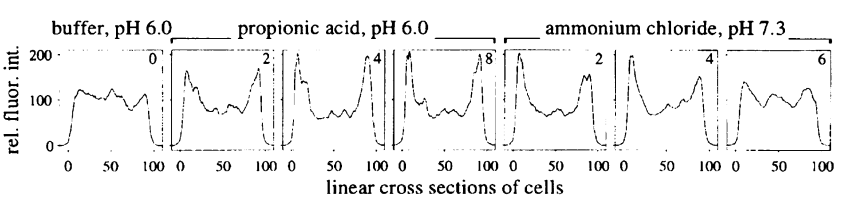

Fig. 7. Time course of the reversible translocation of Gly^2-HsII–GFP between the cytoplasm and surface regions of cells. To cells equilibrated with 20 mM MES buffer (0), pH 6.0, 10 mM propionic acid was added without changing the extracellular pH. Subsequently, this mixture was partially replaced by 20 mM Tris with ammonium chloride, resulting in a pH of 7.3 and a final concentration of 5 mM ammonium chloride. Numbers in the panels refer to minutes after the addition of propionic acid or ammonium chloride, respectively. In a microscopic field the same 10 cells were scanned through the entire sequence. Data were normalized and averaged as for Figure 6.

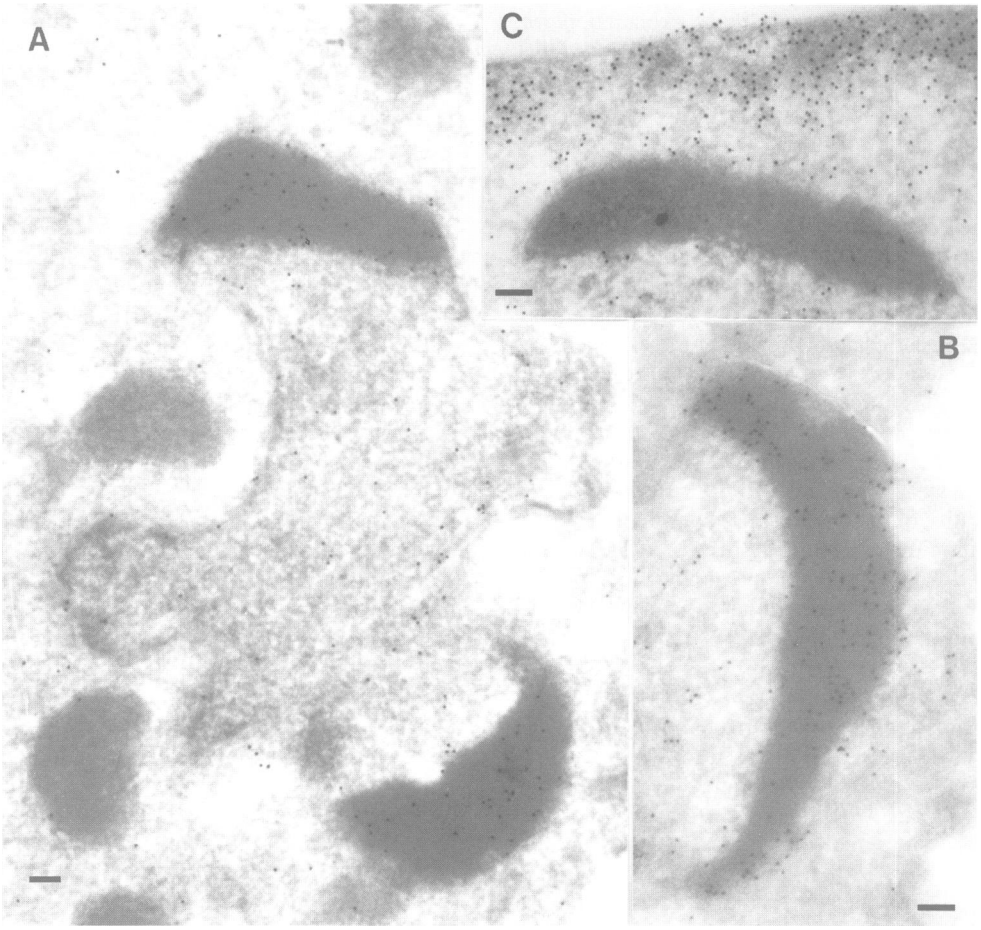

Fig. 8. Nuclei immunogold labelled with anti-hisactophilin antibody (**A** and **B**) or, as a control, with anti-actin antibody (**C**). Cells were pre-treated with propionic acid, and cryosections were labelled with the same antibodies as in Figure 4. Intranuclear localization of hisactophilins is indicated by strong labelling of the nucleoli in (A) and (B), and also by labelling of the nuclear matrix in (A). Two mitochondria on the left of (A) are unlabelled. Specificity of labelling is demonstrated by the absence of gold particles from the nucleoli after labelling with anti-actin antibody, which strongly labelled the cortical region on top of (C). Bars: 100 nm.

are capable of shuttling on a time scale of minutes, not only between cytoplasm and plasma membrane, but also between cytoplasm and the intranuclear compartment.

The import of proteins with a size of 50 kDa or more into the nucleus depends on the exposure on their surface of nuclear localization signals, which are represented by continuous or interrupted stretches of basic amino acids (for review, see Melchior and Gerace, 1995). The exit of proteins from the nucleus to the cytoplasm is determined primarily by their binding to components of the nuclear matrix or the nucleoli (Schmidt-Zachmann *et al.*, 1993). In the light of these data, the strong and rapid accumulation of hisactophilin II–GFP fusion proteins in the nucleus, as seen in Figure 9, was unexpected. These proteins have a size of 40 kDa, close to the upper limit for passing the pores in the nuclear membrane by diffusion, and they lack any canonical continuous or bipartite nuclear localization signal. Nevertheless, the proteins become substantially enriched in the nuclei within <1 min of adding a weak acid to the medium.

In hisactophilins, histidine residues are clustered in loops on the surface of the molecules (Habazettl *et al.*, 1992). The histidine stretches in the hisactophilin II (EMBL/GenBank accession no. 13671), as well as in the hisactophilin I sequence (Scheel *et al.*, 1989), are reminiscent of the arrangement of lysine or arginine residues in continuous or bipartite nuclear localization signals: T^{23}HHGHHDHHTHFHI; S^{64}HHLHGDHSLFHLEHHHGKVSIKGHHHHY; S^{104}HHHDHHA. These data suggest that the histidine stretches function as facultative nuclear localization signals that are switched on in their cationic state. In this state, histidine clusters might act like lysine–arginine stretches which target the protein to the nucleus. After translocation into the nucleus, hisactophilin II apparently binds in its cationic state to negatively charged nuclear constituents. Enrichment is strongest in the nucleoli, which contain densely packed ribosomal DNA and RNA.

A functional relevance of hisactophilin accumulation in the nucleus is suggested by the finding that, in mammalian cells, DNA replication is extremely pH sensitive (Moolenaar, 1986). Hisactophilins or related proteins might contribute to pH homeostasis in the intranuclear space by acting as buffers.

pH sensor proteins as putative secondary messengers and as probes for protein translocation

The peculiar pH sensitivity of hisactophilin shuttling raises the question of the relevance of pH sensing in responses

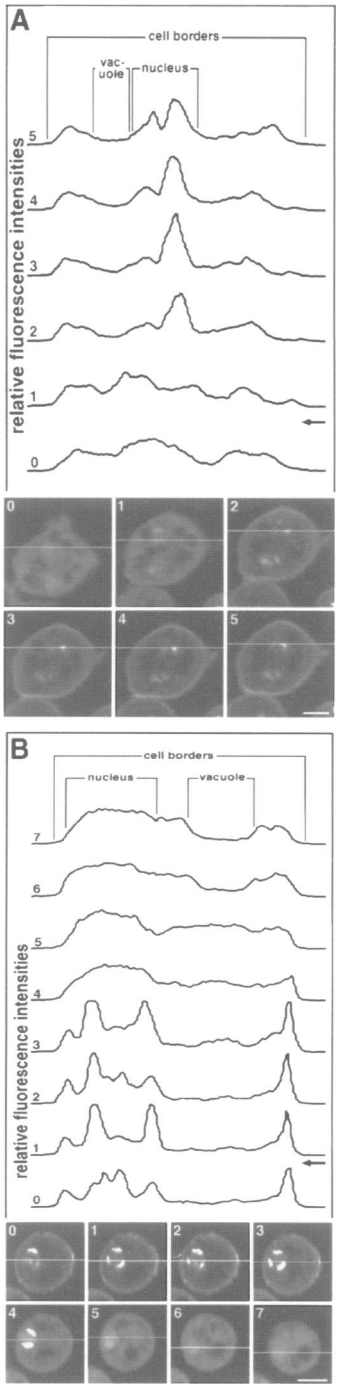

Fig. 9. Dynamics of the shuttling of HsII–GFP fusion proteins between the cytoplasm and nucleus. (**A**) Translocation of Gly^2-HsII–GFP into nuclei after the addition of 10 mM propionic acid at pH 6.0. (**B**) Exit of Ala^2-HsII–GFP from the nucleus after partial replacement of the medium to reach pH 7.3 in the presence of 5 mM ammonium chloride. These examples were chosen to represent both Gly^2- and Ala^2-HsII–GFP; we were unable to distinguish single runs obtained with either one of these fusion proteins. Conditions were the same as in Figure 7. Top panels: sequences of scans, each sequence through a single cell. Numbers indicate scans obtained at intervals of 40 s. Bottom panels: confocal images through the cells scanned on top, horizontal lines showing orientation of the scans relative to positions of the nuclei. Nucleoli are clearly seen as light spots. The propionic acid was added in (A) and ammonium chloride in (B) within 10 s before scan number 1 (arrows).

of cells to external signals. The activation of epithelial or platelet-derived growth factor receptors is known to cause pH shifts of 0.1–0.3 units in the cytoplasm (Moolenaar, 1986). In human neutrophils, chemotactic stimulation causes a rise in intracellular pH, and this shift appears to be involved in regulating the locomotor response (Simchowitz and Cragoe, 1986). In *D.discoideum*, stimulation of cells by the chemoattractant cAMP causes an increase in the intracellular pH (Aerts *et al.*, 1987), resulting in an increased speed of locomotion (Van Duijn and Inouye, 1991). cAMP acts not only as a chemoattractant in *D.discoideum* but also as a signal that regulates gene transcription during development (Williams, 1991). Propionic acid, as well as the proton pump inhibitor diethylstilbestrol, increases the ratio of stalk cells to spores in a population of differentiating *D.discoideum* cells (Gross *et al.*, 1983). Ammonia, which drives hisactophilin II to re-translocate to the cytoplasm, has multiple effects on the development of *D.discoideum* (Sternfeld and David, 1979; Williams *et al.*, 1984; Town *et al.*, 1987; Williams, 1991; Davies *et al.*, 1993). These effects fit into the concept that, in some cases, intracellular pH changes have a secondary messenger function (Busa, 1986). This function is evident in sea urchin fertilization, where a pH change acts as a trigger for development (Johnson *et al.*, 1976). This pH change is important for re-organization of the cytoskeleton after fertilization: it is implicated in the formation of actin bundles in the microvilli of the zygote (Begg *et al.*, 1982).

Subcellular localization of transcription factors is often regulated by charges introduced by phosphorylation (Whiteside and Goodbourn, 1993). The question is whether shuttling of histidine-rich transcription factors between cytoplasm and nucleus can be controlled by altering charges through a pH switch. For instance, the translocation of histidine-rich transcription factors to the nucleus might be favoured or hindered by slight changes in cytoplasmic pH. Candidate proteins of this class include the sex-determining factor from mouse (Coward *et al.*, 1994) and transcription factors which contain $(HX)_n$ repeats (Janknecht *et al.*, 1991).

Finally, we wish to refer to the experimental possibility that sequence motifs of the histidine-rich loops, as they are exposed on hisactophilin molecules (Habazettl *et al.*, 1992), may be fused to other proteins with the prospect of manipulating their nuclear localization from the outside of living cells by slightly changing the cytoplasmic pH. An intriguing perspective is to construct triple fusions of hisactophilin, GFP and a third protein to measure the kinetics of transport through nuclear membrane pores in both directions as a function of the structure and size of a protein.

Materials and methods

Cultivation of D.discoideum

Cells of *D.discoideum* strain AX2-214 or transformants derived from this strain were cultivated axenically at 23°C in liquid nutrient medium on a gyratory shaker at 150 r.p.m., harvested during exponential growth and washed three times in 17 mM K/Na phosphate buffer, pH 6.0, as described by Brink *et al.* (1990). Clones of HsII–GFP- or GFP-producing transformants were cultivated as described for AX2 but under a selection pressure of 20 μg/ml of geneticin (G418).

For purification of the fusion proteins, cells of transformants were

cultivated up to a density of ~5×10^6 cells/ml, and washed cells lysed in homogenization buffer [30 mM Tris–HCl, 4 mM EGTA, 2 mM EDTA, 2 mM dithiothreitol (DTT), 5 mM benzamidine, 30% sucrose, pH 8.0] by nitrogen cavitation in a Parr bomb after equilibration at 950 p.s.i. for 15 min.

Vector construction and transfection of AX2 cells

The vectors for expression of HsII–GFP fusion proteins were based on the pDd-A15-gfp vector (Gerisch *et al.*, 1995), a derivative of pDd-Gal15 (Harwood and Drury, 1990). The actin15 promoter region was exchanged for the corresponding region from pDEXRH (Faix *et al.*, 1992) which gives rise to translation products that contain no foreign N-terminal amino acids. Subsequently, the wild-type cDNA of hisactophilin II, or a sequence mutated by PCR to encode Ala^2 instead of Gly^2, was introduced into *Eco*RI–*Bgl*II sites. Oligonucleotides coding for a flexible $(GlyGlySer)_4$ spacer (Weissman and Kim, 1992) were finally ligated between the Gly^2- or Ala^2-HsII sequence and the coding sequence of GFP (Prasher *et al.*, 1992; Chalfie *et al.*, 1994). The constructs were cloned in *Escherichia coli* JM105 and JM109. AX2-214 cells were transfected according to Nellen *et al.* (1984), and transformants selected with 20 μg/ml of G418.

Purification of GFP and HsII–GFP fusion proteins

Cell lysates were fractionated by centrifugation for 30 min at 10 000 *g* and for 3 h at 100 000 *g*. From the supernatant fraction, GFP or HsII–GFPs were purified by chromatography on DE52 cellulose (Whatman, Biosystems Inc., Clifton, NJ) and Sephacryl S-300 (Pharmacia, Uppsala, Sweden) as described by Scheel *et al.* (1989). Fractions containing GFP or HsII–GFPs were detected according to their green fluorescence by excitation with UV light.

HPLC on a RP18 Lichrospher column (125×4 mm; Merck, Darmstadt, Germany) was performed using pump 420 and detector 430 (Kontron Instruments, München, Germany) at a wavelength of 206 nm. Fusion proteins were analysed in a linear gradient of 0–80% solvent B [0.1% trifluoroacetic acid (TFA; Sigma) in acetonitrile (Lichrosolv, Merck)] in solvent A (0.1% TFA in water) at a flow rate of 1 ml/min.

Mass spectrometry and amino acid sequencing

Masses were determined using an API-III electrospray mass spectrometer (Sciex, Perkin Elmer, Branchburg, NJ) either by direct infusion of proteins separated by HPLC or by on-line reversed-phase HPLC on an Aquapore OD 300, 7 μm, 50×1 mm column (Applied Biosystems). The solvents were 0.1% TFA in water (solvent A) and 0.1% TFA in acetonitrile (solvent B). A linear gradient of 0–80% B in A in 80 min was applied at a flow rate of 50 μl/min with a split to the mass spectrometer of 5 μl/min.

N-terminal sequencing was performed on a pulsed liquid phase sequencer 477 equipped with an on-line PTH analyser 120A (Applied Biosystems).

Co-sedimentation assays

Purified GFP, Gly^2-HsII–GFP or Ala^2-HsII–GFP were used for co-sedimentation assays with actin at concentrations of 1 μM in 20 mM HEPES, adjusted to pH values between 6.0 and 8.0 in 2 mM $MgCl_2$, 1 mM DTT, 1 mM EGTA. G-Actin was purified from *D.discoideum* as described by Spudich (1974), and added to the incubation mixture at a final concentration of 4 μM. Prior to use, all protein solutions were cleared by centrifugation for 30 min at 110 000 *g* at 4°C. The samples were incubated for 30 min at 21°C. Then 100 mM KCl was added and incubation continued for another 30 min to achieve complete actin polymerization. After centrifugation for 30 min at 110 000 *g* at 4°C, supernatants and pellets were separated. The pellets were resuspended in 400 μl of buffer containing 100 mM HEPES, 100 mM KCl, 2 mM $MgCl_2$, 1 mM DTT and 1 mM EGTA, pH 8.0. The supernatants were adjusted to the same volume and buffer conditions as the pellets, and fluorescence was determined at 470 nm for excitation and 505 nm for emission using an SFM25 spectrofluorimeter (Kontron).

Manipulation of pH conditions

Cells were harvested at a density of 1×10^6 cells/ml, washed in Na/K phosphate buffer, pH 6.0, resuspended in 2 ml of the buffer and allowed to adhere on a large glass coverslip on which was fixed a plastic ring of 40 mm diameter. Prior to the experiments with differing buffer conditions, the cells were incubated for 15 min in the appropriate MES or Tris buffer (2 ml of 20 mM MES, pH 6.0, or 2 ml of 20 mM Tris–HCl, pH 8.0).

To manipulate the cytoplasmic pH, 1 ml of buffer was replaced by either 1 ml of 20 mM MES buffer, pH 6.0, containing 20 (or 40) mM propionic acid, or by 1 ml of 20 mM Tris buffer, pH 8.0, containing 20 mM ammonium chloride. For continuously recording the same cells under changing buffer conditions, the effect of propionic acid in MES buffer, pH 6.0, was reversed by twice adding 1 ml of ammonium chloride in Tris buffer, pH 8.0, to achieve a final concentration of 10 mM ammonium chloride and a buffer pH of 7.3 ± 0.1.

Image acquisition and analysis

GFP fluorescence was examined by confocal microscopy (ZEISS LSM 410) at an optical slice thickness of ~1 μm. For excitation, the 488 nm argon ion laser line was used combined with a dichroic mirror (510 nm) and an LP520 emission filter (ZEISS). The cells were scanned every 40 s with a scanning time of 32 s to achieve a compromise between distortion of the image due to cell and particle movement and noise suppression in the signal. Contrast and brightness were adjusted to fit into the range of 256 grey levels of the digitizer.

Images were analysed using the Applied Visualization System (AVS 5.01, Advanced Visual Systems, Waltham, MA) running at a DEC-Alpha 3000/600 with 160 Mbyte RAM. Series of confocal images were read directly into the AVS by a program designed to analyse the parameter set coded in the TIFF files of the ZEISS microscope. Images from the AVS were printed in true-colour TIFF format at a PC using COREL-DRAW software (Corel Corporation, Ontario, Canada) and a thermo-sublimation printer (Tektronix Phaser II SD, Wilsonville, OR).

For the calculation of fluorescence intensity distributions, pixel intensities were extracted along an adjustable line that crosses the cell. For averaging intensity distributions, line scans from 10–60 cells were normalized with respect to the cell diameter, then averaged, and normalized according to the integral of the intensity.

Antibody labelling

For the localization of endogenous hisactophilins, AX2 cells were fixed for 15 min at room temperature in saturated picric acid solution/2% formaldehyde in 10 mM PIPES–HCl (15:85, v/v) at pH 6.0 or pH 8.0, in accord with the pH of incubation (Humbel and Biegelmann, 1992). For fluorescence microscopy, the cells were incubated with anti-hisactophilin mAb 54-11-10, and labelled with TRITC-conjugated goat anti-mouse IgG (Jackson ImmunoResearch, West Grove, PA, code 115-025-062). For electron microscopy, the fixed cells were embedded in gelatine, blocks infused with 1.8 M sucrose in 15% polyvinylpyrrolidone, and specimens cryosectioned essentially as described by Tokuyasu (1989). Sections of ~70 nm thickness were pre-incubated with 2% fish gelatine, and incubated overnight with either 10 μg/ml of anti-hisactophilin mAb 54-11-10 (Scheel *et al.*, 1989) or 5 μg/ml of anti-actin mAb 224-236-1, kindly provided by Bettina Mühlbauer. Subsequently, the sections were incubated with 9 μg/ml of rabbit anti-mouse IgG (Jackson Immuno-Research, code 315-005-048) and labelled with protein A–10 nm gold (BioCell, Cardiff, UK), diluted 1:50. Sections were post-fixed with 2% glutaraldehyde, stained with uranyl acetate in methylcellulose acccording to Griffiths (1993) and micrographs taken in a JEM-100CX transmission electron microscope (JEOL).

Acknowledgements

We thank Rob Kay and Steve Hodgkinson, MRC Cambridge, and Jan Faix for vectors, Markus Maniak and Annette Müller-Taubenberger for instructions and Gerald Marriott for reading the manuscript.

References

Aerts,R., De Wit,R. and Van Lookeren Campagne,M. (1987) Cyclic AMP induces a transient alkalinization in *Dictyostelium*. *FEBS Lett.*, **220**, 366–370.

Begg,D.A., Rebhun,L.I. and Hyatt,H. (1982) Structural organization of actin in the sea urchin egg cortex: microvillar elongation in the absence of actin filament bundle formation. *J. Cell Biol.*, **93**, 24–32.

Behrisch,A., Dietrich,Ch., Noegel,A.A., Schleicher,M. and Sackmann,E. (1995) The actin-binding protein hisactophilin binds *in vitro* to partially charged membranes and mediates actin coupling to membranes. *Biochemistry*, **34**, 15182–15190.

Brink,M., Gerisch,G., Isenberg,G., Noegel,A.A., Segall,J.E., Wallraff,E. and Schleicher,M. (1990) A *Dictyostelium* mutant lacking an F-actin crosslinking protein, the 120 kDa gelation factor. *J. Cell Biol.*, **111**, 1477–1489.

Busa,W.B. (1986) Mechanisms and consequences of pH-mediated cell regulation. *Annu. Rev. Physiol.*, **48**, 389–402.

Chalfie,M., Tu,Y., Euskirchen,G., Ward,W.W. and Prasher,D.C. (1994) Green fluorescent protein as a marker for gene expression. *Science*, **263**, 802–804.

Cohen,S.M., Knecht,D., Lodish,H.F. and Loomis,W.F. (1986) DNA sequences required for expression of a *Dictyostelium* actin gene. *EMBO J.*, **5**, 3361–3366.

Coward,P., Nagai,K., Chen,D., Thomas,H.D., Nagamine,C.M. and Lau,Y.-F.C. (1994) Polymorphism of a CAG trinucleotide repeat within *Sry* correlates with B6.Y^{Dom} sex reversal. *Nature Genet.*, **6**, 245–250.

Davies,L., Satre,M., Martin,J.-B. and Gross,J.D. (1993) The target of ammonia action in *Dictyostelium*. *Cell*, **75**, 321–327.

Edmonds,B.T., Murray,J. and Condeelis,J. (1995) pH regulation of the F-actin binding properties of *Dictyostelium* elongation factor 1α. *J. Biol. Chem.*, **270**, 15222–15230.

Faix,J., Gerisch,G. and Noegel,A.A. (1992) Overexpression of the csA cell adhesion molecule under its own cAMP-regulated promoter impairs morphogenesis in *Dictyostelium*. *J. Cell Sci.*, **102**, 203–214.

Fukui,Y. (1978) Intranuclear actin bundles induced by dimethyl sulfoxide in interphase nucleus of *Dictyostelium*. *J. Cell Biol.*, **76**, 146–157.

Gerisch,G., Albrecht,R., Heizer,C., Hodkinson,S. and Maniak,M. (1995) Chemoattractant-controlled accumulation of coronin at the leading edge of *Dictyostelium* cells: monitoring using a green fluorescent protein–coronin fusion protein. *Curr. Biol.*, **5**, 1280–1285.

Griffiths,G. (1993) *Fine Structure Immunocytochemistry*. Springer, Berlin.

Gross,J.D., Bradbury,J., Kay,R.R. and Peacey,M.J. (1983) Intracellular pH and the control of cell differentiation in *Dictyostelium discoideum*. *Nature*, **303**, 244–245.

Habazettl,J., Gondol,D., Wiltscheck,R., Otlewski,J., Schleicher,M. and Holak,T.A. (1992) Structure of hisactophilin is similar to interleukin-1 beta and fibroblast growth factor. *Nature*, **359**, 855–858.

Hanakam,F., Eckerskorn,Ch., Lottspeich,F., Müller-Taubenberger,A., Schäfer,W. and Gerisch,G. (1995) The pH-sensitive actin-binding protein hisactophilin of *Dictyostelium* exists in two isoforms which both are myristoylated and distributed between plasma membrane and cytoplasm. *J. Biol. Chem.*, **270**, 596–602.

Hanakam,F., Gerisch,G., Lotz,S., Aet,T. and Seelig,A. (1996) Binding of hisactophilin I and II to lipid membranes is controlled by a pH dependent myristoyl-histidine switch. *Biochemistry*, in press.

Harwood,A.J. and Drury,L. (1990) New vectors for expression of the *E.coli lacZ* gene in *Dictyostelium*. *Nucleic Acids Res.*, **18**, 4292.

Humbel,B.M. and Biegelmann,E. (1992) A preparation protocol for postembedding immunoelectron microscopy of *Dictyostelium discoideum* with monoclonal antibodies. *Scanning Microsc.*, **6**, 817–825.

Inouye,K. (1989) Regulation of cytoplasmic pH in the differentiating cell types of the cellular slime mold *Dictyostelium discoideum*. *Biochim. Biophys. Acta*, **1012**, 64–68.

Janknecht,R., Sander,C. and Pongs,O. (1991) (HX)n repeats: a pH-controlled protein–protein interaction motif of eukaryotic transcription factors? *FEBS Lett.*, **295**, 1–2.

Johnson,J.J., Epel,D. and Paul,M. (1976) Intracellular pH and activation of sea urchin eggs after fertilization. *Nature*, **262**, 661–664.

Kim,J., Mosior,M., Chung,L.A., Wu,H. and McLaughlin,S. (1991) Binding of peptides with basic residues to membranes containing acidic phospholipids. *Biophys. J.*, **60**, 135–148.

Kim,J., Blackshear,P.J., Johnson,J.D. and McLaughlin,S. (1994) Phosphorylation reverses the membrane association of peptides that correspond to the basic domains of MARCKS and neuromodulin. *Biophys. J.*, **67**, 227–237.

McLaughlin,S. and Aderem,A. (1995) The myristoyl-electrostatic switch: a modulator of reversible protein–membrane interactions. *Trends Biochem. Sci.*, **20**, 272–276.

Melchior,F. and Gerace,L. (1995) Mechanisms of nuclear protein import. *Curr. Opin. Cell Biol.*, **7**, 310–318.

Moolenar,W.H. (1986) Effects of growth factors on intracellular pH regulation. *Annu. Rev. Physiol.*, **48**, 363–376.

Nellen,W., Silan,C. and Firtel,R.A. (1984) DNA-mediated transformation in *Dictyostelium discoideum*: regulated expression of an actin gene fusion. *Mol. Cell. Biol.*, **4**, 2890–2898.

Nunnally,M.H. and Craig,S.W. (1980) Small changes in pH within the physiological range cause large changes in the consistency of actin–filamin mixtures. *J. Cell Biol.*, **87**, 218a.

Prasher,D.C., Eckenrode,V.K., Ward,W.W., Prendergast,F.G. and Cormier,M.J. (1992) Primary structure of the *Aequorea victoria* green-fluorescent protein. *Gene*, **111**, 229–233.

Randazzo,P.A., Terui,T., Sturch,S., Fales,H.M., Ferrige,A.G. and Kahn,R. (1995) The myristoylated amino terminus of ADP-ribosylation factor 1 is a phospholipid- and GTP-sensitive switch. *J. Biol. Chem.*, **270**, 14809–14815.

Resh,M.D. (1994) Myristoylation and palmitoylation of Src family members: the fats of the matter. *Cell*, **76**, 411–413.

Scheel,J., Ziegelbauer,K., Kupke,T., Humbel,B.M., Noegel,A.A., Gerisch,G. and Schleicher,M. (1989) Hisactophilin, a histidine-rich actin-binding protein from *Dictyostelium discoideum*. *J. Biol. Chem.*, **264**, 2832–2839.

Schmidt,J.M., Robson,R.M., Zhang,J. and Stromer,M.H. (1993) The marked pH dependence of the talin–actin interaction. *Biochem. Biophys. Res. Commun.*, **197**, 660–666.

Schmidt-Zachmann,M.S., Dargemont,C., Kühn,L.C. and Nigg,E.A. (1993) Nuclear export of proteins: the role of nuclear retention. *Cell*, **74**, 493–504.

Simchowitz,L. and Cragoe,E.J.,Jr (1986) Regulation of human neutrophil chemotaxis by intracellular pH. *J. Biol. Chem.*, **261**, 6492–6500.

Spudich,J.A. (1974) Biochemical and structural studies of actomyosin-like proteins from non-muscle cells. II. Purification, properties and membrane association of actin from amoebae of *Dictyostelium discoideum*. *J. Biol. Chem.*, **249**, 6013–6020.

Sternfeld,J. and David,Ch.N. (1979) Ammonia plus another factor are necessary for differentiation in submerged clumps of *Dictyostelium*. *J. Cell Sci.*, **38**, 181–191.

Swierczynski,S.L. and Blackshear,P.J. (1995) Membrane association of the myristoylated alanine-rich C kinase substrate (MARCKS) protein. *J. Biol. Chem.*, **270**, 13436–13445.

Tanaka,T., Ames,J.B., Harvey,T.S., Stryer,L. and Ikura,M. (1995) Sequestration of the membrane-targeting myristoyl group of recoverin in the calcium-free state. *Nature*, **376**, 444–447.

Tokuyasu,K.T. (1989) Use of poly(vinylpyrrolidone) and poly(vinyl alcohol) for cryoultramicrotomy. *Histochem. J.*, **21**, 163–171.

Town,C.D., Dominov,J.A, Karpinski,B.A. and Jentoft,J.E. (1987) Relationships between extracellular pH, intracellular pH, and gene expression in *Dictyostelium discoideum*. *Devel. Biol.*, **122**, 354–362.

Van Duijn,B. and Inouye,K. (1991) Regulation of movement speed by intracellular pH during *Dictyostelium discoideum* chemotaxis. *Proc. Natl Acad. Sci. USA*, **88**, 4951–4955.

Vergères,G., Manenti,S., Weber,T. and Stürzinger,C. (1995) The myristoyl moiety of myristoylated alanine-rich C-kinase substrate (MARCKS) and MARCKS-related protein is embedded in the membrane. *J. Biol. Chem.*, **34**, 19879–19887.

Weissman,J.S. and Kim,P.S. (1992) The pro region of BPTI facilitates folding. *Cell*, **71**, 841–851.

Whiteside,S. and Goodbourn,S. (1993) Signal transduction and nuclear targeting: regulation of transcription factor activity by subcellular localisation. *J. Cell Sci.*, **104**, 949–955.

Williams,G.B. (1991) Regulation of cellular differentiation during *Dictyostelium* morphogenesis. *Curr. Opin. Genet. Dev.*, **1**, 358–362.

Williams,G.B., Elder,E.M. and Sussmann,M. (1984) Modulation of the cAMP relay in *Dictyostelium discoideum* by ammonia and other metabolites: possible morphogenetic consequences. *Devel. Biol.*, **105**, 377–388.

Zheng,J., Knighton,D.R., Xuong,N.H., Taylor,S.S., Sowadski,J.M. and Eyck,L.F.T. (1993) Crystal structures of the myristoylated catalytic subunit of cAMP-dependent protein kinase reveal open and closed conformations. *Protein Sci.*, **2**, 1559–1573.

Received on January 9, 1996; revised on February 15, 1996